Evaluation of Sound Transmission Models for Automotive Applications

Maria Gavila Lloret[1], Ulrich Gabbert[2], Gregor Müller[1]

[1] *BMW AG, 80788 München, Deutschland, Email: Maria.Gavila-Lloret@bmw.de*

[2] *Otto-von-Guericke-Universität Magdeburg, 39106 Magdeburg, Deutschland*

Introduction

Acoustics is a distinctive feature for premium class vehicles. However, some of the current trends in the automotive industry may have a negative impact on the acoustic performance, such as weight reduction and engine down-sizing. Moreover, the introduction of electric and autonomous cars exposes the users to new perceivable noise sources. In order to bring a competitive product to the market, with a satisfying balance of the comfort requirements and the weight and costs limitations, it is needed to complement measurements with simulative processes. The final objective of an ongoing investigation is the development of a model that predicts the airborne sound propagation phenomena from the engine, through the firewall and the dashboard, to the passenger cabin.

One key factor to achieve reliable results lies on an accurate modeling of the several noise control treatments (NCT). A large number of these acoustic treatments is made of poroelastic components, whose acoustical effectiveness is directly related to the amount of energy that they are able to dissipate. Energy losses within a poroelastic material are mainly driven by viscous friction of the fluid inside the pores, structural damping of the solid frame, and thermal exchange between the two phases. A detailed microscopical description of all these phenomena, even if possible, is not applicable for a real size problem, mainly due to its excessive cost. Instead, it is preferable to represent the material as an homogenized compound with a highly complex dissipative behavior. A short review of some of these homogenization techniques is presented in this article, including different formulations for the finite element method and the statistical energy analysis. Their performance is compared on three simplified setups, and some conclusions regarding their applicability are presented.

Theoretical background

This section summarizes the analyzed approaches for the representation of poroelastic components.

Finite Element Method (FEM, [1])

Two main approaches for modeling poroelastic media are found within the framework of the finite element method:

- Full poroelastic description, which solves Biot's poroelasticity equations for both solid and fluid phases of the material.
- Equivalent fluid representation, where the visco-inertial coupling between the phases is neglected and only the fluid inside the pores is computed.

Equivalent fluid models can be divided in rigid frame (if the stiffness of the skeleton is large) and limp frame (if the inertial coupling is considered by modifying the density of the equivalent fluid). In the commercial FE software *LMS Virtual.Lab* different formulations are available. The Johnson-Champoux-Allard (JCA) model ([2], [3], is a semi-phenomenological model and can be used in combination with an elastic frame (for the full poroelastic computation), and with limp or rigid frames. The Delany-Bazley-Miki (DBM) model [4] is based on empirical data and works with limp and rigid frame, and the Craggs model [5] was derived for rigid skeleton materials.

The main drawback associated with FE is its elevated computational effort: each node has 4 degrees of freedom for the full poroelastic model, and the number of required elements increases with the frequency.

Statistical Energy Analysis (SEA, [6])

To deal with this inherent problem of the FEM, energetic approaches as the SEA may be used. This method predicts average sound and vibration levels. Analogue to the thermal exchange problem, the power balance between subsystems is proportional to the difference in their modal energies and coupling loss factors, whereas the dissipated energy in a subsystem is proportional to its damping loss factor.

In the SEA frame, a noise control treatment is represented by its impedance, computed from the combination of explicit mathematical models for the behavior of each layer. The introduction of a NCT modifies the coupling and damping loss factor of the subsystem to which is attached.

Another possibility is the employment of a hybrid approach, where SEA and FEM components are combined. In the following examples, a hybrid model has been built by substituting in a energetic model the plate component by its finite element counterpart.

Test setup

In order to assess the efficiency of the aforementioned methods, two different multi-layered systems have been selected. The properties of each configuration are listed in the Table 1. Configuration 1 has a smaller size to speed up the computation times, while the size of Configuration 2 should enable the direct comparing with measured results. Standard values for the steel properties are used, whereas the properties for the heavy layers and the foams come from experimental data.

Both systems have been analyzed in 3 different states,

Table 1: Tested configurations

Configuration 1 Size: $0.5m \times 0.5m$		Configuration 2 Size: $1m \times 1m$	
$0.8mm$	Steel	$0.75mm$	Steel
$14mm$	Foam 1	$10.8mm$	Foam 2
$3kg/m^2$	Heavy Layer	$4kg/m^2$	Heavy Layer

namely the foam layer alone, the foam attached to the steel plate, and lastly a spring-mass system built by the steel plate, the foam and the heavy layer. This last one could be a simplified representation of a real system used in automotive applications (e.g. firewall with spring-mass). All setups are placed between two semi-infinite fluids under a diffuse field acoustic excitation, and the transmission loss (TL, eq. 1) of the system in every case is computed for frequencies between 80Hz and 2000Hz, range in which engine radiation through the firewall has its largest contribution.

$$\mathrm{TL} = 10 \log_{10} \ 1/\tau = 10 \log_{10} \ \Pi_{\mathrm{in}}/\Pi_{\mathrm{out}} \qquad (1)$$

Results

Next, some of the obtained results are commented.

Foam layer

Figure 1 shows the FE results for the transmission loss of a foam layer in the Configuration 1. The case where the foam layer is modeled as a full poroelastic component serves as reference, since this formulation is the only one which solves both phases in the medium, and is designated in the graphs by *JCA elastic*. The other results belong to equivalent fluid models.

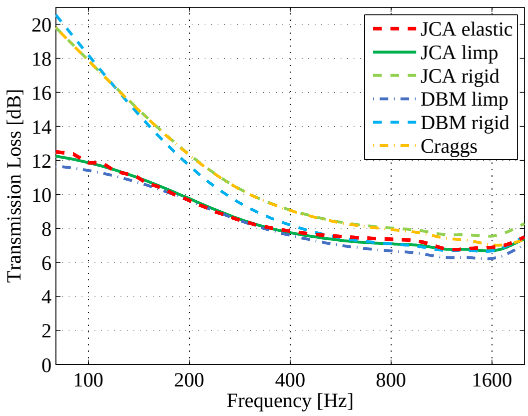

Figure 1: Transmission loss for a foam layer under diffuse field excitation (Config. 1).

One interesting feature when solving the FE equations is the possibility to compute the dissipated power inside the poroelastic material and to separate into the different dissipation mechanisms taking place (i.e. viscous effects in the fluid, structural damping, thermal exchanges, viscous effects in the solid, or viscous effects due to the fluid-structure couplings). For this application most of the sound energy is dissipated due to viscous losses in the fluid phase (over 80% above 150Hz). At lower frequencies, the energy loss due to structural damping has also a noticeable share, whereas the percentage of thermal dissipation increases slightly with the frequency. This energy distribution explains the good match between the elastic and limp models, because the main mechanisms are well captured, whereas the rigid frame formulations tend asymptotically towards the full poroelastic results.

Since only the pressure degree of freedom is solved in the equivalent fluid formulations (in contrast to the four degrees of freedom of the full poroelastic), the computation time can be reduced by a factor between 3 and 8, depending on the relative size of the model components, without affecting accuracy.

Plate with foam layer

Next, the foam layer is attached to a steel plate, on which the diffuse sound field is applied. Results in this section refer to Configuration 2. Under these conditions, the frame of the foam is directly excited and most of the power is dissipated by structural damping in the frame (see Figure 2). In this case, the contribution of the dissipation in the fluid phase is comparatively small, but it is because the chosen material has a large structural damping coefficient, $\eta_s \approx 0.3$. When this factor is reduced, the energy dissipation distributes more uniformly between the structural damping and the viscous losses in the fluid phase.

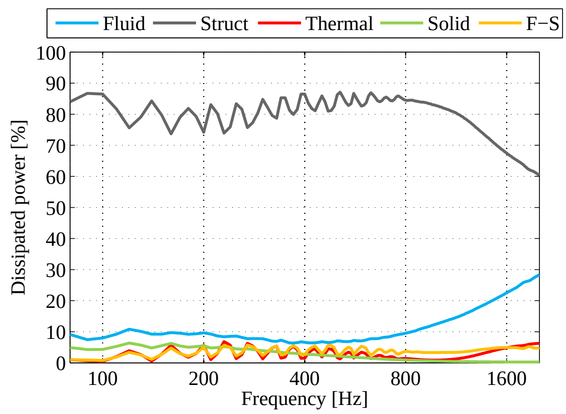

Figure 2: Percentage of dissipated power by each mechanism inside the foam layer bonded on to a plate (Config. 2).

Figure 3 shows the transmission loss FE results for this configuration. Additionally, the results for the bare steel plate are displayed (*Plate*). Comparing firstly the solutions for the plate and the full poroelastic formulation, one can observe that, at the low frequency range, the introduction of the foam layer produces a shift of the resonances towards lower frequencies and an increase of the TL values. This effect is reproduced if the foam is substituted by an increase of the plate density, corresponding to the additional mass provided by the foam. Limp and rigid models cannot reproduce this impact because the additional damping of the frame is neglected.

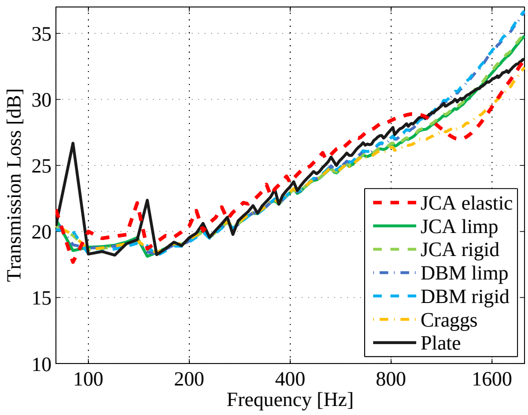

Figure 3: Transmission loss for a foam bonded on to a plate under diffuse field excitation (Config. 2).

Plate with spring-mass system

In this case, the results for both configurations are discussed. Figure 4 gives interesting information about the energy dissipation inside the foam layer of Configuration 1. For frequencies comprised around 300Hz and 500Hz, the effect of the viscous losses in the fluid decreases and the structural damping and the viscous coupling losses play a dominant role, which corresponds to the frequency range where the spring-mass resonance occurs.

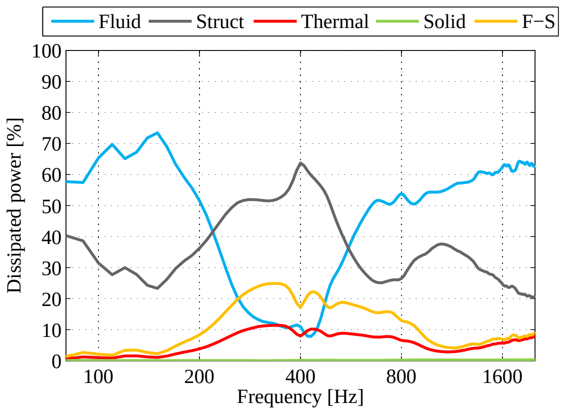

Figure 4: Percentage of dissipated power by each mechanism inside the foam layer bonded on to a plate (Config. 1).

Finite element rigid and limp frame models are compared to the full poroelastic solution in the Figure 5. Except for the Craggs formulation, all the other models show a shift of the resonance frequency of the spring-mass system towards lower values. This effect is due to the fact that the presence of the solid frame increases the dynamic stiffness of the material, but this cannot be reproduced in the equivalent fluid formulations.

For this system, SEA and hybrid results have also been computed using *ESI VA One*. The results are displayed in Figure 6 and together with with the FE computations for the JCA elastic formulation. The comparison with the energetic and hybrid models proves that the asymptotic behavior at the higher frequencies is the same for

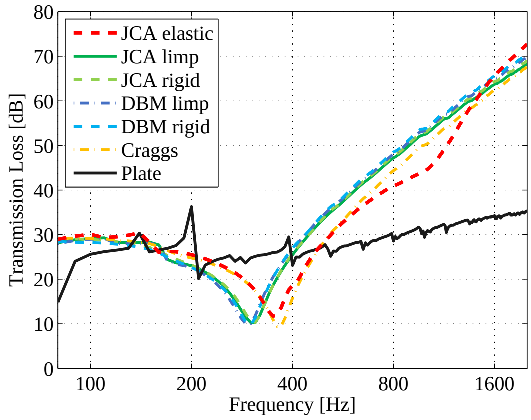

Figure 5: Transmission loss for a spring-mass system bonded on to a plate under diffuse field excitation (Config. 1).

the different formulations. On the lower frequency range some discrepancies are observed, especially for the complete SEA formulation, since it is not suitable in this frequency range where the modal density is low.

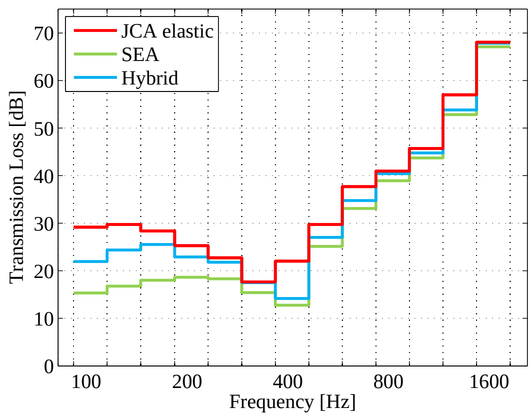

Figure 6: Transmission loss for a spring-mass system bonded on to a plate under diffuse field excitation (Config. 1).

Figure 7 reproduces the results of the FE simulations for the Configuration 2. Main differences from Configuration 1 are, on the one hand, that the spring-mass resonance peak is less pronounced for the full poroelastic model and, on the other hand, that the structural damping is the dominating dissipation mechanism (the distribution is very similar to that of the plate-foam system in Figure 2). Both facts can be explained by the high damping factor of the studied foam, only captured with JCA elastic.

Comparison with measurement results

In the following step, the accuracy of the proposed modeling approaches is tested by confronting the simulation results with some experimental data. To this effect, the spring-mass system of Configuration 2 was placed in a window test bench. In an attempt to reduce the influence of the experimental mounting conditions, the insertion loss (equation 2) is computed in this case, and the obtained results for the finite element method with JCA elastic frame, the SEA model, the hybrid approach and

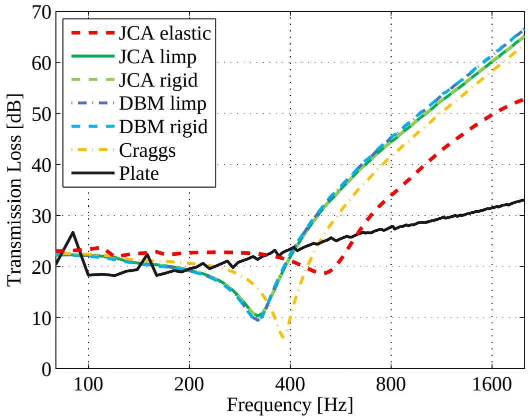

Figure 7: Transmission loss for a spring-mass system bonded on to a plate under diffuse field excitation (Config. 2).

the experimental setup are plotted in Figure 8.

$$\mathrm{IL} = \mathrm{TL}_{\mathrm{NCT}} - \mathrm{TL}_{\mathrm{plate}} = \Pi_{\mathrm{out,plate}} - \Pi_{\mathrm{out,NCT}} \qquad (2)$$

There is good match among the simulative results. However, the agreement with the measured values is not satisfactory and further investigations regarding the parameters' influence, mounting conditions and with other materials and excitation sources are being carried out.

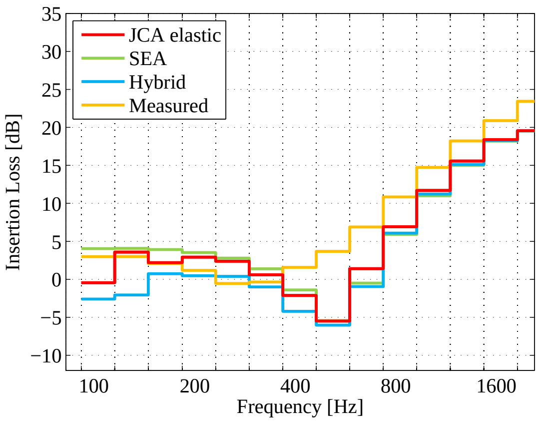

Figure 8: Insertion loss for a spring-mass system bonded on to a plate. Comparison with experimental data (Config. 2).

Conclusions and overview

Though poroelastic materials are widely applied as noise control treatments, there exists no definite approach for their modeling that has a complete range of validity.

Equivalent fluid models imply a notable reduction of the required model size, because the equivalent fluid wavelength is always larger than the shortest wavelength in the poroelastic media, and of the computation time, since only the interstitial pressure needs to be solved. However, they are not longer valid in cases where the porous material is directly coupled to a excited structure, because it directly induces vibrations in the skeleton and, therefore, the assumption of motionless frame would neglect the dissipation due to the structural damping. As seen in the proposed examples, the power loss in the frame can be the main dissipation mechanism for some materials. Therefore, the application of equivalent fluid formulations is recommended only for absorbers, that is, components directly excited by an airborne wave.

Approaches based on energetic methods, such as the statistical energy analysis, are advantageous in the higher frequency range, as the size of the model is independent of the frequency. However, since they are based on frequency and component averages, their applicability is restricted if local results are necessary.

A good compromise may be found in the use of hybrid approaches, either by combining discretized and energy-based components (as shown in the previous examples), or by dividing the frequency range in two parts and selecting the most suitable method for each case [6].

Even if it was not the topic of this article, it should be mentioned that another difficulty regarding the proposed methods arises from the obtainment of the material parameters. The determination of most poroelastic properties requires special measurement methods, and the boundary conditions under which the tests are carried out may have a big influence the results. For this reason, other approaches to describe these materials could also be of interest, for instance experimentally determined transfer matrices [8].

References

[1] Allard, J. F., Atalla N.: Propagation of Sound in Porous Media. Modeling Sound Absorbing Materials, 2nd ed. Wiley, Chichester, UK, 2009

[2] Johnson D. L., *et al.*: Theory of dynamic permeability and tortuosity in fluid-saturated porous media. J. Fluid Mech. 176 (1987), 379-402

[3] Champoux Y., Allard J.-F.: Dynamic tortuosity and bulk modulus in air-saturated porous media. J. Appl. Phys. 70 (1991), 1975-1979

[4] Miki, Y.: Acoustical properties of porous materials - Modifications of Delany-Bazley models. J. Acoust. Soc. Japan 11-1 (1990), 19-24

[5] Craggs, A.: A Finite Element Model for rigid porous absorbing materials. J. Sound Vib. 61 (1978), 101-111

[6] Desmet, W., Pluymers, B., Atak, O. (Editors): 'MID-FREQUENCY' - CAE Methodologies for Mid-frequency analysis in vibrations and acoustics. KU Leuven, Heverlee, Belgium, 2012

[7] Panneton, R., Atalla, N.: Numerical prediction of sound transmission through finite multilayer systems with poroelastic materials. J. Acoust. Soc. Am. 100-1 (1996), 346-354

[8] Veronesi, G., *et al.*: Patch Transfer Function Approach for Analysis of Coupled Vibro-Acoustic Problems Involving Porous Materials. SAE Tech. Paper 2014-01-2092 (2014)